Available online at www.sciencedirect.com
SCIENCE DIRECT®
Physics Letters A 339 (2005) 207–211
PHYSICS LETTERS A
www.elsevier.com/locate/pla

Wigner bosonic molecules with repulsive interactions and harmonic confinement

P. Capuzzi [a,*], N.H. March [b,c], M.P. Tosi [a]

[a] *NEST-INFM and Classe di Scienze, Scuola Normale Superiore, Piazza dei Cavalieri 7, I-56126 Pisa, Italy*
[b] *Department of Physics, University of Antwerp, 171 Groenenborgerlaan, B-2020 Antwerp, Belgium*
[c] *Oxford University, Oxford, England, UK*

Received 16 February 2005; accepted 22 February 2005

Available online 21 March 2005

Communicated by V.M. Agranovich

Abstract

In earlier work, the momentum distribution of harmonically confined bosons has been calculated for interparticle interactions which are also harmonic for an arbitrary number N of repelling Bose particles. After a brief discussion of the pair function in this model, attention is also given, but now for $N = 2$, to the single-particle density for the repulsive interaction potential λ/r_{12}^2, where r_{12} is the interboson distance and λ the repulsive coupling strength. The single-particle density is displayed for specific values of λ, with attention focusing on the limit of strong repulsive coupling. Throughout, the focus is on the fingerprints of Wigner bosonic molecules.

Keywords: Wigner bosonic molecules; Exactly solvable models; Harmonic confinement; Harmonic interactions

In earlier work [1], attention has been focused on the momentum distribution of harmonically confined bosons for interparticle interactions which also have harmonic form for an arbitrary number N of repelling (and also attracting) Bose particles. In this Letter, following a brief discussion of the pair correlation function $P(\mathbf{r}_1, \mathbf{r}_2)$ in this model, attention is also given, but now for $N = 2$, to the single-particle density $\rho(r)$ for the repulsive interaction potential changed to the form λ/r_{12}^2 where $r_{12} = |\mathbf{r}_1 - \mathbf{r}_2|$ denotes the interboson separation while λ measures the repulsive coupling strength. In particular, the ground-state particle density $\rho(r)$ is displayed for specific values of λ, with attention focusing on the change from the Gaussian form of $\rho(r)$ as λ goes from zero to large values of this repulsive coupling strength. It will be shown that $\rho(r)$ for large λ already contains clear fingerprints of the formation of a Wigner bosonic molecule.

Following the culture of the background to the present study, let us utilize the early work of Cohen

* Corresponding author.
E-mail address: capuzzi@sns.it (P. Capuzzi).

0375-9601/$ – see front matter
doi:10.1016/j.physleta.2005.02.078

and Lee [2] on the low-order density matrices for N bosons with harmonic confinement and also harmonic interparticle repulsion. In particular, from Eq. (2.35) of [2] for the second-order density matrix, we can write the diagonal pair function $P(\mathbf{r}_1, \mathbf{r}_2)$ already referred to above as

$$P(\mathbf{r}_1, \mathbf{r}_2) = \frac{N(N-1)}{2} \left\{ \frac{N\omega\delta_N^2/\pi^2}{(N-2)\omega + 2\delta_N} \right\}^{3/2} \times \exp\{-2b_1(r_1^2 + r_2^2) - 2b_2\mathbf{r}_1 \cdot \mathbf{r}_2 + b_3(2\mathbf{r}_1 \cdot \mathbf{r}_2 + r_1^2 + r_2^2)\}, \quad (1)$$

where b_1–b_3 are recorded explicitly in Eqs. (2.38)–(2.40) of [2]. Finally, $\delta_N^2 = \omega^2 \pm N\gamma^2$, where the confinement potential V is $\frac{1}{2}\omega^2 r^2$ and the interaction potential is $\pm\frac{1}{2}\gamma^2 r_{ij}^2$. The limit of strong repulsions is achieved for $\delta_N \simeq 0$ and a further increase of γ would break the external confinement. The important point here is the appearance in Eq. (1), via the scalar product $\mathbf{r}_1 \cdot \mathbf{r}_2$, of the angle between the position vectors $\mathbf{r}_1$ and $\mathbf{r}_2$, superposed of course on 'confinement' terms of the expected Gaussian form. If we fix particle 1 say at position $(0, 0, a)$ in Cartesian coordinates, then the top panel in Fig. 1 displays $P([0, 0, a], \mathbf{r}_2)$ to demonstrate this conditional probability distribution of boson separation for two bosons. For large bosonic repulsion, the tendency towards 'particle localization' is becoming evident. The effect of repulsions is more clearly seen in the behavior of the pair function $g([0, 0, a], \mathbf{r}_2)$, defined as

$$g(\mathbf{r}_1, \mathbf{r}_2) = \frac{2N}{N-1} \frac{P(\mathbf{r}_1, \mathbf{r}_2)}{\rho(\mathbf{r}_1)\rho(\mathbf{r}_2)}. \quad (2)$$

For non-interacting particles $g(\mathbf{r}_1, \mathbf{r}_2) \equiv 1$ reflecting the absence of correlations, while on switching on the interactions g develops a peak at $\mathbf{r}_2 = (\delta_N + \omega)/(\delta_N - \omega)\mathbf{r}_1$, which tends to $\mathbf{r}_2 = -\mathbf{r}_1$ in the limit of strong interactions. This is accompanied with a diminution of the width of g along the direction of $\mathbf{r}_1 - \mathbf{r}_2$. The location of the peaks is expected since, given a particle at $\mathbf{r}_1$, in order to minimize the energy at large interparticle repulsions, r_{12} must be maximal and thus $\mathbf{r}_2 = -\mathbf{r}_1$. These effects are illustrated in the bottom panel of Fig. 1.

We have also considered the distributions of 4 and 6 bosons with interparticle harmonic repulsions. In this case g has a maximum when

$$\mathbf{r}_2 = \frac{\delta_N + (N-1)\omega}{\delta_N - \omega}\mathbf{r}_1, \quad (3)$$

however, its width is non-monotonic on increasing the strength of the interaction, diverging for extremely low values of δ_N. This suggests that, in contrast to the two-boson problem, the spatial distribution of 4 or 6 bosons does not possess a structure at large couplings. In Fig. 2 we show contour plots of P for $N = 2, 4$ and 6 bosons and two values of the interparticle interaction close to the strong repulsion limit. The contour plots evince the strongly elongated structure of the pair function for two bosons at $\delta_N \simeq 0$ and illustrate the regular behavior of the distributions of 4 and 6 particles on increasing δ_N. However, we stress here that the ground-state density $\rho(r)$ retains its spherical Gaussian form for all N, though naturally the half-width of the Gaussian depends on the strength of the interparticle interactions. These comments parallel those pertaining to the momentum distribution in [1].

This is the point to consider the alternative choice of interparticle repulsion energy λ/r_{12}^2. Here we can draw on the work of Crandall et al. [3]. While these authors were concerned exclusively with a two-electron atomic model, with therefore no reference to bosons, we can utilize the fact that they have an exact, spatially symmetric solution of the Schrödinger equation for confinement potential $V(r)$ given by

$$V(r) = \frac{1}{2}m\omega^2 r^2, \quad (4)$$

and repulsive interaction potential energy $W(r_{12})$ given by

$$W(r_{12}) = \lambda/r_{12}^2, \quad \lambda > 0. \quad (5)$$

The nodeless solution which they utilize for their two-electron atomic model, times of course a singlet spin function to give an overall antisymmetric fermion wave function, has the unnormalized form [3, Eq. (3.14)]

$$\Psi(\mathbf{r}_1, \mathbf{r}_2) = e^{-m\omega r_1^2/2\hbar} e^{-m\omega r_2^2/2\hbar} r_{12}^{\alpha}, \quad (6)$$

where $\alpha = [(1 + 4\lambda m/\hbar^2)^{1/2} - 1]/2$. Clearly, when the interparticle repulsion is switched off in the present bosonic application, the $r_{12} \equiv |\mathbf{r}_1 - \mathbf{r}_2|$ term in (6) is replaced by unity and one has an elementary product wave function in which the two bosons under

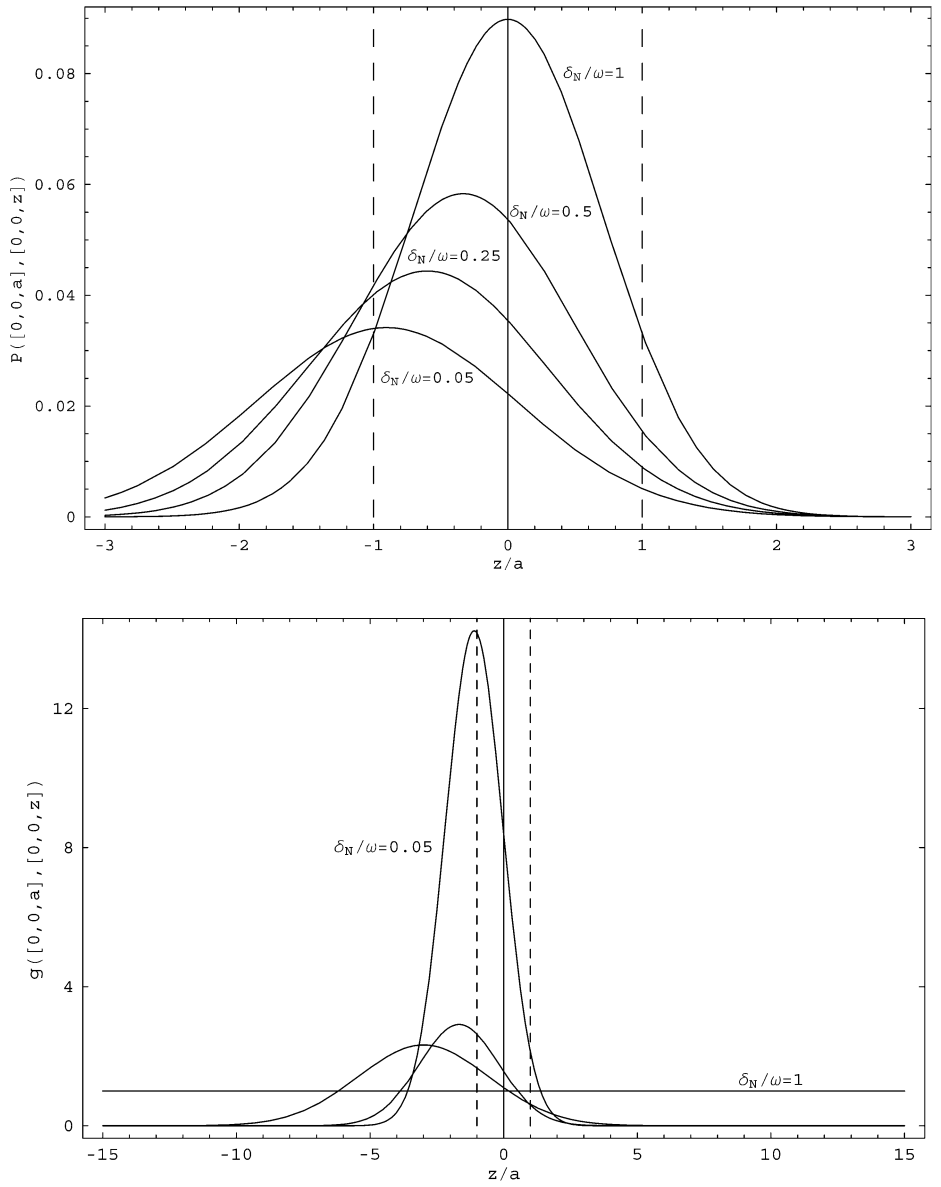

Fig. 1. Pair functions $P(\mathbf{r}_1, \mathbf{r}_2)$ (top panel) and $g(\mathbf{r}_1, \mathbf{r}_2)$ (bottom panel) for $\mathbf{r}_1 = a\hat{z}$ and $\mathbf{r}_2 = z\hat{z}$ of two bosons interacting with harmonic repulsions as functions of z/a. The different curves correspond to the values of $\delta_N/\omega = 1$, 0.5, 0.25 and 0.05. The dashed lines locate $|z_1| = a$.

discussion occupy the same Gaussian orbital. While, of course, we can immediately construct $P(\mathbf{r}_1, \mathbf{r}_2)$, after appropriate normalization, as $|\Psi(\mathbf{r}_1, \mathbf{r}_2)|^2$ from Eq. (6), we shall rather start displaying below the single-particle density given by

$$\rho(r) = \mathcal{N} \int \Psi^2(\mathbf{r}_1, \mathbf{r}_2)\, d\mathbf{r}_2, \tag{7}$$

where $\mathcal{N}$ is to be chosen such that

$$\int \rho(r)\, d\mathbf{r} = 2 \tag{8}$$

in the present two-boson model. Explicitly, using Eq. (6) in Eq. (7), we have

$$\rho(r) = \mathcal{N} e^{-m\omega r^2/\hbar} \int e^{-m\omega r_2^2/\hbar} |\mathbf{r} - \mathbf{r}_2|^{2\alpha}\, d\mathbf{r}_2. \tag{9}$$

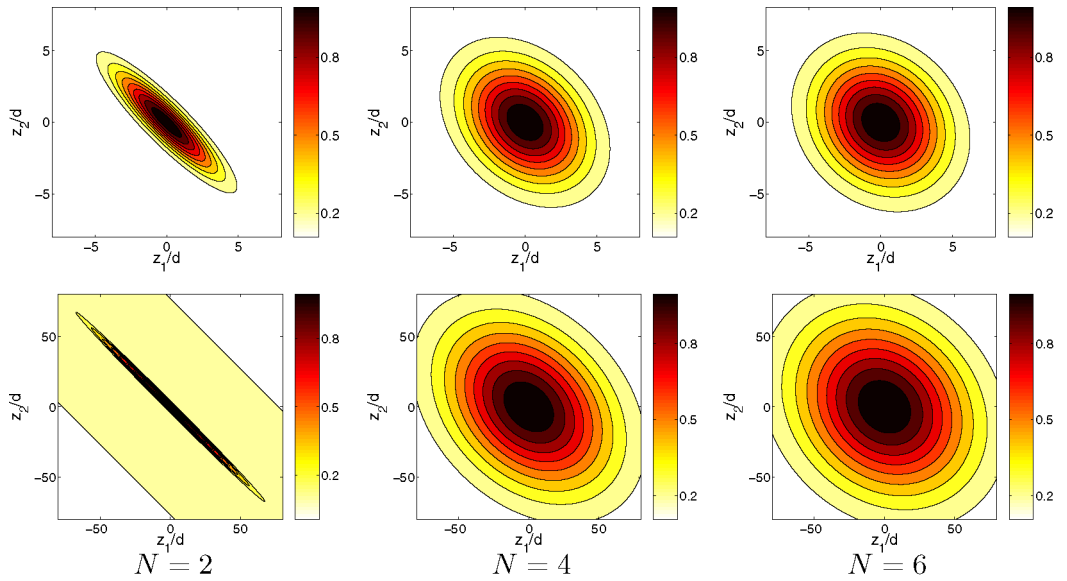

Fig. 2. Contour plots of the pair functions $P([0,0,z_1],[0,0,z_2])$ as functions of z_1/d and z_2/d with $d=\sqrt{\hbar/(m\omega)}$ for N bosons interacting with the harmonic potential $\frac{1}{2}\omega^2 r^2$. The left, middle and right columns correspond to $N=2$, 4 and 6 bosons respectively, and the top and bottom rows to $\delta_N/\omega = 0.05$ and 10^{-3}.

The integral entering Eq. (9) gives

$$\rho(r) = \frac{2^{1-\alpha}}{\pi^{3/2}}\left(\frac{m\omega}{\hbar}\right)^{3/2} \times e^{-2m\omega r^2/\hbar}\,{}_1F_1\left(\tfrac{3}{2}+\alpha, \tfrac{3}{2}, \tfrac{m\omega r^2}{\hbar}\right), \tag{10}$$

where ${}_1F_1$ is the confluent hypergeometric function [4]. For discrete values of λ given by

$$\left[\left(1+\frac{4\lambda m}{\hbar^2}\right)^{1/2} - 1\right] = 2n, \tag{11}$$

where n is an integer, $\rho(r)$ can be explicitly written as $\exp(-m\omega r^2/\hbar)$ times a polynomial of order $2n$. In practice, $\rho(r)$ has to be evaluated numerically and sample results for $\rho(r)$ are displayed in Fig. 3. The repulsive interaction between the two bosons, first widens the density profile and then leads to the formation of a maximum displaced from the trap center. This can be viewed as the first signature of the formation of a Wigner molecule of bosonic particles.

Let us now examine the pair function for two bosons with λ/r_{12}^2 repulsion. In Fig. 4 we show the contour plots of $|\Psi(\mathbf{r}_1,\mathbf{r}_2)|^2$ for $\alpha = 0.1$ and 10. We observe the appearance of two well separated regions where the conditional probability is maximum. From these plots it is clear that the probability distribution for the distance between the two particles is a highly peaked function around

$$r_{12}^0/d = \sqrt{2+2\alpha}, \tag{12}$$

where $d=\sqrt{\hbar/(m\omega)}$. Furthermore, the differences with the harmonic repulsions are notable. Even though we found that the probability distribution of two bosons is maximum when they are in opposite positions, their repulsion is not as strong as to separate them from each other at a minimum distance as two bosons interacting with λ/r_{12}^2 are. In this sense, the lack of strong localization can be attributed to the weak interactions present in the exact model of harmonic interactions.

To conclude, it is of interest to make contact with the numerical study of Romanovsky et al. [5]. Though these workers considered different repulsive interactions, namely, contact and Coulomb, from those studied in the present Letter, some similarities are evident. However, we have only $N=2$ for the inverse square interaction potential λ/r_{12}^2, whereas the numerical studies of [5] considered $N=6$. For Coulomb repulsions, they noted, in two dimensions, in contrast to the present three-dimensional study, the tendency to

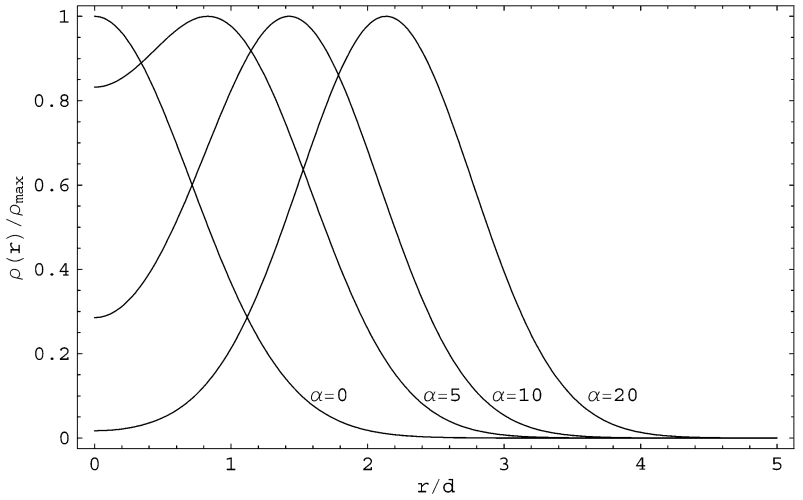

Fig. 3. Boson densities $\rho(r)/\rho_{\max}$ for two bosons with the λ/r_{12}^2 interaction potential as functions of r/d with $\rho_{\max}$ the maximum density for given α, and $d = \sqrt{\hbar/(m\omega)}$. The different lines correspond to different values of α (measuring the strength of the repulsive interaction: see Eq. (6)) as indicated in the plot.

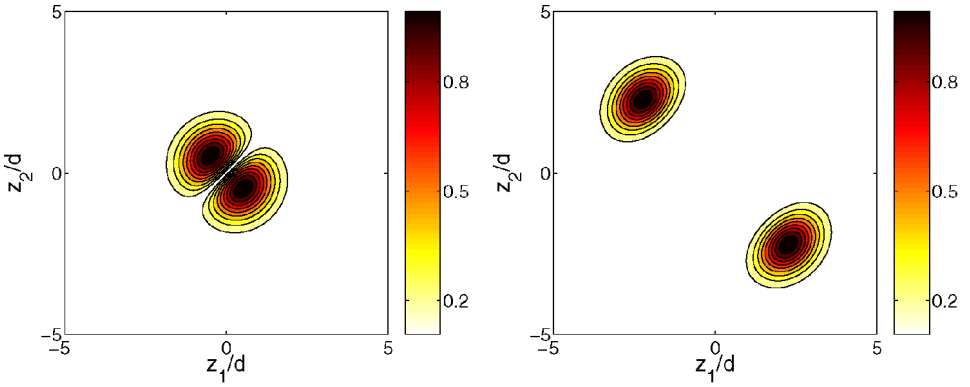

Fig. 4. Contour plots of the pair functions $P([0,0,z_1],[0,0,z_2])$ as functions of z_1/d and z_2/d for two bosons interacting with the λ/r_{12}^2 potential. Left and right panels correspond to $\alpha = 0.1$ and 10, respectively.

ring formation of the bosons, with, as they term it, a breaking of rotational symmetry.

Acknowledgements

This work has been partially supported by an Advanced Research Initiative of Scuola Normale Superiore di Pisa (SNS) and by the Istituto Nazionale di Fisica della Materia (INFM). N.H. March acknowledges that his contribution to this Letter was largely made during a visit to SNS in 2005. He wishes to thank SNS for the very stimulating atmosphere where this study was carried out and for generous support.

References

[1] N.H. March, M.P. Tosi, Phys. Chem. Liq. 39 (2001) 183.
[2] L. Cohen, C. Lee, J. Math. Phys. 26 (1985) 3105.
[3] R. Crandall, R. Whitnell, R. Bettega, Am. J. Phys. 52 (1984) 438.
[4] M. Abramowitz, I.A. Stegun (Eds.), Handbook of Mathematical Functions with Formulas, Graphs, and Mathematical Tables, Dover, New York, 1972.
[5] I. Romanovsky, C. Yannouleas, U. Landman, Phys. Rev. Lett. 93 (2004) 230405.